Supplementary material for the article:

Stanković, I. M.; Blagojević Filipović, J. P.; Zarić, S. D. Carbohydrate – Protein Aromatic Ring Interactions beyond CH/π Interactions: A Protein Data Bank Survey and Quantum Chemical Calculations. *Int. J. Biol. Macromol.* **2020**, *157*, 1–9.
https://doi.org/10.1016/j.ijbiomac.2020.03.251

**Supplemental information**

# CARBOHYDRATE – PROTEIN AROMATIC RING INTERACTIONS BEYOND CH/π INTERACTIONS: A PROTEIN DATA BANK SURVEY AND QUANTUM CHEMICAL CALCULATIONS

**Ivana M. Stanković, Jelena P. Blagojević Filipović, and Snežana D. Zarić**

Figure S1. The example of a and b carbohydrate faces, β-D-glucose.

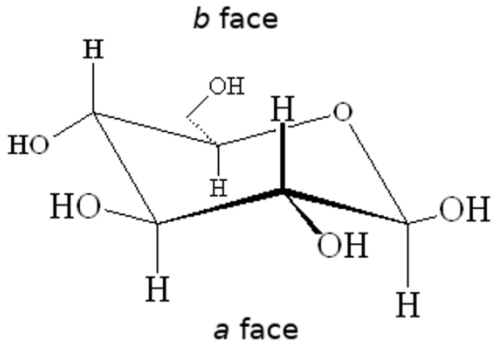


The contacts with CH/O interactions, where aromatic amino acids are hydrogen donors are prone to larger dihedral angle and offset values (Figure S2). There is no particular tendency for contacts with CH/O interactions, where carbohydrates are hydrogen donors (Figure S2). Figures S3-S5 show that smaller dihedral angle and offset values are more common for contacts with CH/N, OH/π and classical hydrogen bonds, respectively.

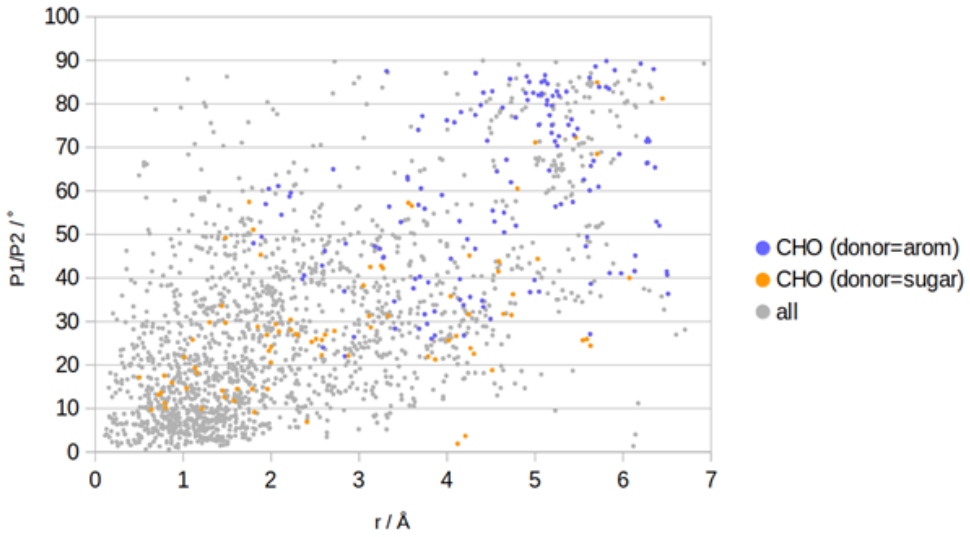


**Figure S2**. Depencences of the angles between rings on offset values, for all contacts and contacts with CH/O interactions, when hydrogen donor is the aromatic amino acid or sugar molecule

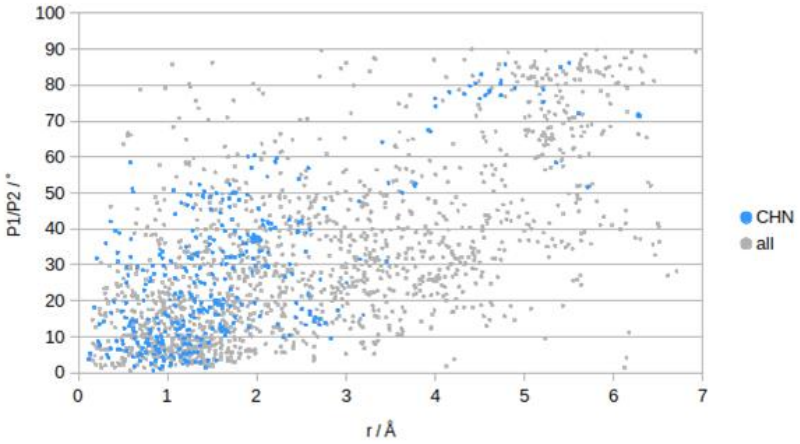


**Figure S3**. Depencences of the angles between rings on offset values, for all contacts and contacts with CH/N interactions

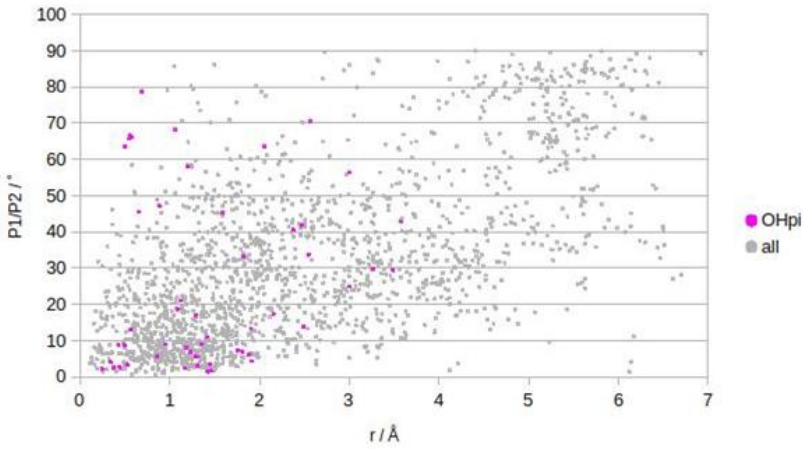

**Figure S4**. Depencences of the angles between rings on offset values, for all contacts and contacts with OH/π interactions

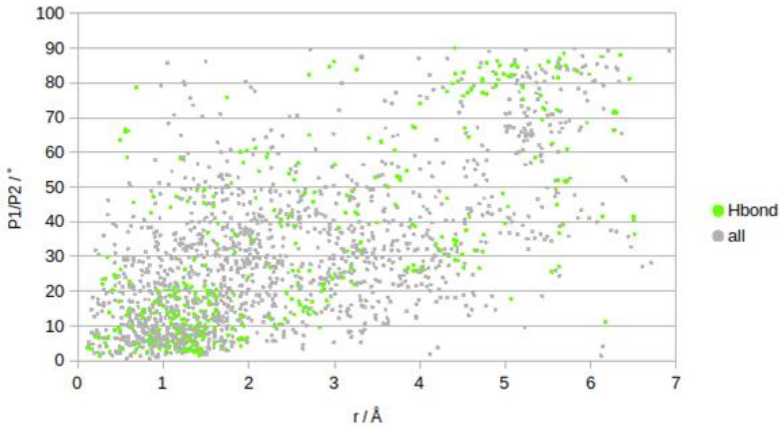


**Figure S5**. Depencences of the angles between rings on offset values, for all contacts and contacts with classical hydrogen bonds

## Higher $P_1/P_2$ angles

The sugar-aromatic contacts involving CH/π interactions tend to be parallel (Figure 2A, 3 and 4), as the consequence of the sugar CH group nearly perpendicular to the sugar plane. However, in some of the contacts there are higher $P_1/P_2$ angles between rings (Figure 2A) that are the consequence of distorted high-energy sugar rings, or deoxy sugars with missing OH groups. The example is shown in Figure S6.

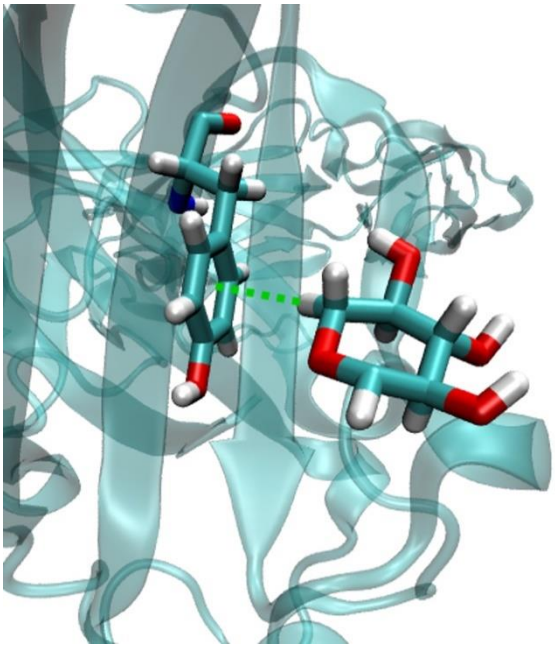

**Figure S6:** An example of the deoxy sugar forming non-parallel contact to the aromatic ring. Green dotted line represents CH/π interaction.

## The distribution of the number of CH/π interactions

The distribution of the number of CH/π interactions per sugar-aromatic pair demonstrates tendency towards only one or two CH/π bonds per sugar-aromatic pair (Figure S7). It means that one or two CH/π bonds per sugar/aromatic pair are sufficient for holding them together. PHE and TYR form only one or two, rarely three CH/π interactions, while TRP can form one, two, three or four because of its two aromatic rings. We plotted R(r) dependences for each one of these groups: with one, two, three or four CH/π interactions (Figure S7). For the higher number of CH/π interactions, the tendency is towards less scattered R values and lower r values, which proves that the CH/π interactions are responsible for tighter bonding between carbohydrate and aromatic moieties, even though one such bond is sufficient for holding the carbohydrate in place.

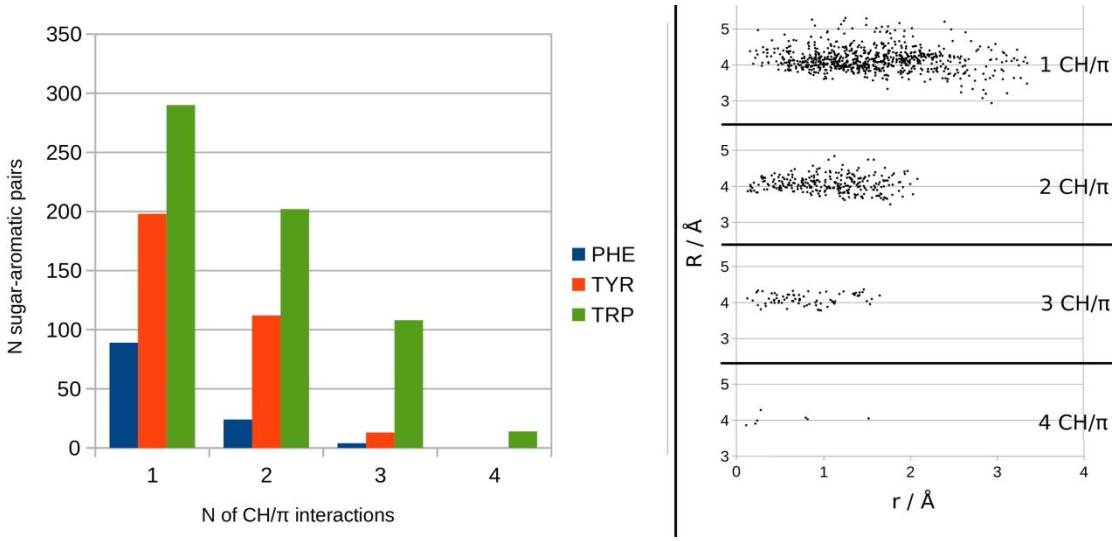


**Figure S7:** The distribution of the number of CH/π interactions per sugar-aromatic pair. The R(r) diagrams related to each number of CH/π interactions are shown on the right side.

## The sandwich aromatic amino acid/carbohydrate arrangements

The survey pointed to rare sandwich arrangements (two aromatics per sugar monomer, Figure S8) for the CH/π interacting pairs: from 1054 contacts with CH/π only 49 of them are positioned in aromatic sandwich.

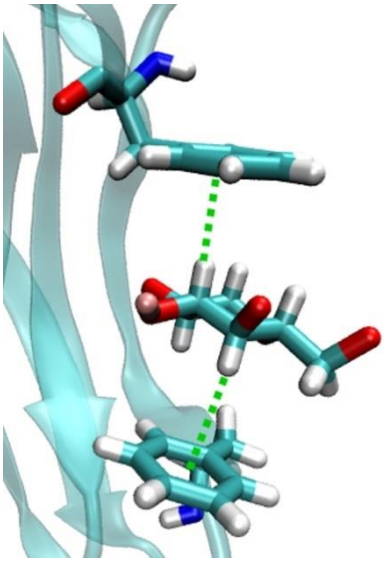

**Figure S8:** Example of sandwich interaction: two aromatic rings interacting simultaneously with one sugar ring. PDB id: 5DPN.

The graphs in Figure S9 represent the projections of monosaccharide centers onto aromatic ring plane of the six-membered rings of PHE, TYR and TRP. Data for contacts with CH/π interactions (Figure S9) show no specificity in offset nor φ angle (Figure 2B), except for TRP. The clustering in the fourth quadrant for TRP is due to interactions with five-membered TRP ring (Figure 2B, Figure S9A). The distribution of the φ angle in contacts without CH/π interactions (Figure S9B) shows that there is clustering in the second and third quadrant for all three aromatic rings, probably due to steric hindrances caused by the protein backbone.

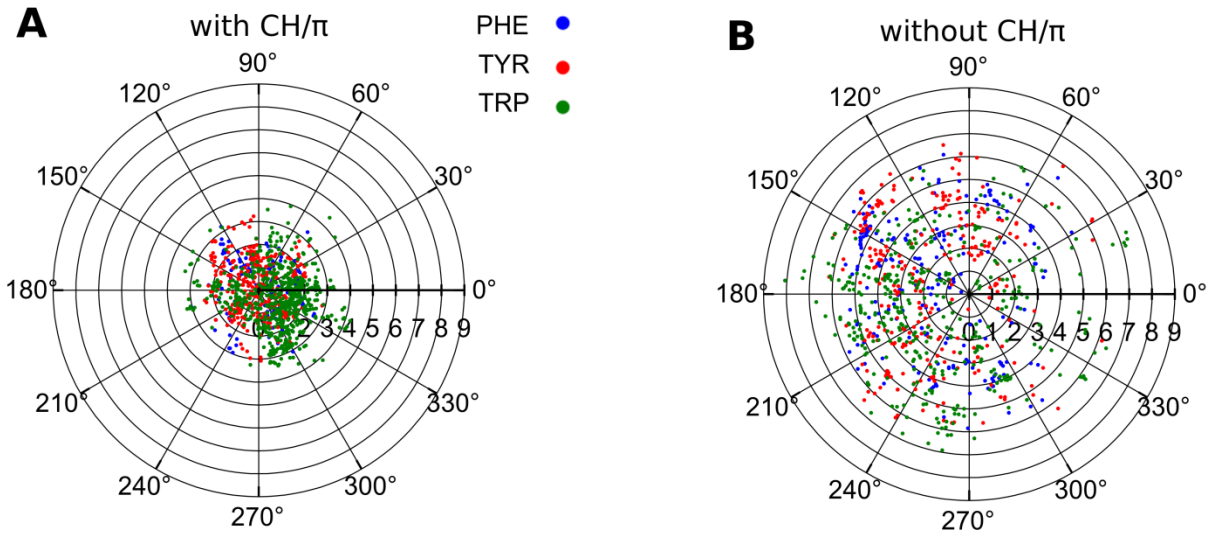


**Figure S9.** The polar graph offset - φ angle (Figure 2B) for the contacts involving CH/π interactions (A) and without CH/π interactions (B). Different aromatic amino acids are represented separately.

**Table S1.** Pattern of the average number of aromatic rings per carbohydrate substrate (both monomers and oligomers) and per monomer, with and without CH/π interactions.

| Number of monomers per oligomer unit | N of substrates | Any contact | | With CH/π | | Without CH/π | |
|---|---|---|---|---|---|---|---|
| | | N of aromatics per substrate | N of aromatics per monomer | N of aromatics per substrate | N of aromatics per monomer | N of aromatics per substrate | N of aromatics per monomer |
| 1 | 799 | 0.68 | 0.68 | 0.32 | 0.32 | 0.36 | 0.36 |
| 2 | 243 | 1.45 | 0.72 | 0.99 | 0.50 | 0.46 | 0.22 |
| 3 | 156 | 1.40 | 0.47 | 0.85 | 0.28 | 0.55 | 0.19 |
| 4 | 95 | 1.92 | 0.48 | 1.33 | 0.33 | 0.59 | 0.15 |
| 5 | 54 | 2.28 | 0.46 | 1.39 | 0.28 | 0.89 | 0.18 |
| 6 | 49 | 3.14 | 0.52 | 1.82 | 0.30 | 1.32 | 0.22 |
| 7 | 26 | 2.78 | 0.40 | 1.62 | 0.23 | 1.16 | 0.17 |
| 8 | 20 | 2.95 | 0.39 | 1.40 | 0.18 | 1.55 | 0.21 |

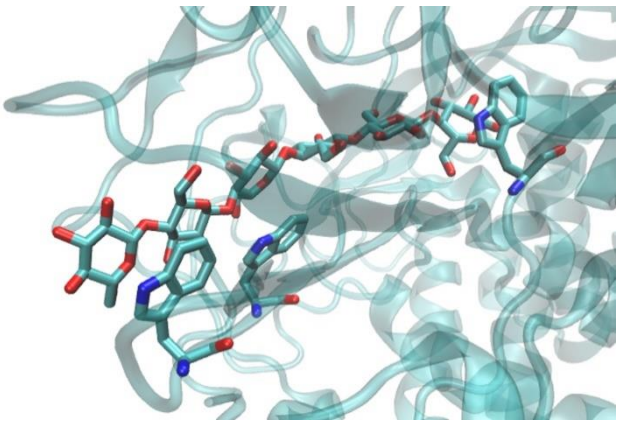

**Figure S10.** An example of a six units long carbohydrate substrate interacting with three aromatic rings in the protein cleft. PDB id: 1L2A.